Temperature Dependence and Annealing Effects in Surface-Enhanced Raman Scattering on Chemically Prepared Silver Island Films

Chan Ho Kwon,[†] Doo Wan Boo,[‡] Hyun Jin Hwang,[§] and Myung Soo Kim*,[†]

Department of Chemistry, Seoul National University, Seoul 151-742, Korea, Department of Chemistry, Yonsei University, Seoul 120-749, Korea, and Department of Chemistry, Kyunghee University, Seoul 130-701, Korea

Received: May 5, 1999; In Final Form: July 29, 1999

The surface-enhanced Raman scattering (SERS) intensities for ethanethiol adsorbed on a silver island film have been measured for a variety of annealing conditions over the 15−300 K temperature range. Reversible temperature dependence of the C−S stretching intensities for an unannealed film similar to the case of 1-propanethiol reported previously was found, with the intensity at 15 K being greater than that at 300 K by a factor of ∼2.5. The preferential SERS enhancement at lower surface temperature, normalized by the value at 300 K, decreased substantially as the silver films were annealed. For example, the relative enhancement factor at 15 K over 300 K after 50 min of annealing at 150 °C was ∼1.2. Such annealing effects on the SERS enhancement were more pronounced at longer wavelengths and during the initial period of annealing. The combined field emission scanning electron microscopy (FE-SEM) and atomic force microscopy (AFM) studies revealed that the annealing of the films induced changes in the morphologies of the islands with increases in the radii and decreases in the heights. From the FE-SEM and AFM images the distributions of the aspect ratios of the island hemispheroids for unannealed and annealed films were determined. The average electromagnetic (EM) enhancement factors for such distributions were calculated using the low-temperature-modified equation for EM enhancement [*J. Phys. Chem. B* **1998**, *102*, 7203]. The excellent agreement between the EM theoretical predictions and the experimental findings strongly suggested that the observed reversible temperature dependence of the SERS enhancement and the annealing effect originated from the inherent temperature dependence and morphology dependence of the EM mechanism in SERS.

1. Introduction

Since the observation of surface-enhanced Raman scattering (SERS) about 20 years ago, it has been widely studied in many research areas such as spectroscopy, surface science, material science, electrochemistry, etc.[1−4] Although the exact origin of the phenomenon is not yet understood, it is generally agreed that the electromagnetic (EM) effect arising from resonant coupling of the surface plasmon excitation with radiation in the presence of surface roughness plays a major role in SERS. During the past 2 decades, many mechanistic studies of SERS using the surfaces of Ag colloids or Ag island films have been conducted but provided only limited information on the origins of the detailed aspects of SERS phenomena because of the ill-characterized size and morphology distributions of Ag nanoparticles. With recent advances in surface-active experimental techniques such as atomic force microscopy (AFM),[5−7] scanning electron microscopy (SEM),[8] scanning tunneling microscopy (STM),[9−11] etc., the distributions of the size and morphology of the Ag nanoparticles can be experimentally measured and the information can be readily used in the SERS experiments to understand the size and morphology effect. These combined SERS and surface characterization studies could provide much valuable information on the various SERS phenomena and furthermore on the collective properties of many Ag particles in SERS. Other significant efforts in this direction are the near-field measurements of SERS on single Ag nanoparticles[12−14] with well-characterized sizes and morphologies, and the results provided unambiguous experimental evidence for the mechanisms of SERS phenomena.

One of the most intriguing aspects in SERS is the recently observed reversible temperature dependence in the SERS intensities with preferential enhancements at lower temperatures. Previously, the observed temperature dependence in the SERS intensities of 1-propanethiol adsorbed on a silver island film was explained qualitatively within the framework of EM theory, particularly using the low-temperature-modified equation[15,16] for EM enhancement following the EM concepts proposed by Leung et al.[17] and Gersten and Nitzan.[18] According to this equation, a large SERS enhancement occurs when the surface plasmon resonance condition is satisfied for the real part of the surface dielectric function (ϵ) (determined mainly by the size and morphologies of Ag nanoparticles), and at the same time the imaginary part of ϵ is small at the excitation wavelength.[19,20] The observed temperature dependence of larger enhancement at lower temperatures was thus attributed to the fact that the imaginary part of ϵ (which appears in the denominator of the equation) is an increasing function of temperature. The calculated temperature dependence of EM enhancement for various sizes and morphologies of islands agreed well with that of experiment. No direct correlation of the theoretical predictions with the experimental findings, however, was possible because of the lack of information on the sizes and morphologies of Ag islands on the film. Therefore, it has been our goal to extend these studies by combining the SERS experiments with the SEM

* To whom correspondence should be sent.
[†] Seoul National University.
[‡] Yonsei University.
[§] Kyunghee University.

10.1021/jp991479o CCC: $18.00
Published on Web 10/14/1999

and AFM studies for determining the distributions of Ag islands on the film. Particularly important would be the investigation of the temperature dependence of SERS enhancement for the systematically varied sizes and morphologies of the islands. Such studies would provide an important platform for testing the validity of the low-temperature-modified EM equation in explaining the temperature dependence in SERS.

For this goal, we have studied the temperature dependence of the C−S stretching SERS intensities for ethanethiol adsorbed on the silver island film over the temperature range 15−300 K as a function of annealing time (a means of changing the island morphologies) and combined these results with the size and morphology distributions of islands characterized by using the field emission SEM (FE-SEM) and AFM techniques. It will be shown that a reversible temperature dependence for the C−S stretching mode of ethanethiol adsorbed on an unannealed film similar to the case of 1-propanethiol was found with greater enhancement at lower temperature. The preferential SERS enhancement at lower temperature, normalized by the value at 300 K, decreased substantially as the silver film was annealed. Such an annealing effect was more pronounced at longer wavelengths and during the initial period of annealing. These new experimental findings are discussed by comparing them with the theoretical predictions based on the low-temperature-modified EM equation.

2. Experimental Procedures

The chemical procedure to prepare the silver island film was previously reported.[21] A sapphire window was chosen as the substrate because of its large thermal conductivity. The substrate was precleaned with nitric acid and was sonicated repeatedly in several solvents before chemical deposition. A silver island film prepared as above was dipped in 1 mM KCl solution for 5−6 min and rinsed with deionized water. This treatment improved the surface quality of the film, such as the mechanical stability and reproducibility of SERS activity. Then the film was dipped in 1 mM ethanethiol solution in methanol for 20 min in order to achieve the full surface coverage. The remaining solution on the film was removed by sufficient rinsing in water. Ethanethiol was purchased from Fluka and was used without further purification. All the chemicals used in this experiment otherwise specified were reagent grade.

A Raman spectrometer (SPEX 1877E) equipped with a liquid nitrogen cooled CCD detector was modified by replacing the filter stage with a holographic super notch filter (Kaiser Optical System) as described previously.[16] A factor of ∼10 improvement in *S*/*N* ratio was achieved by this modification. This allows data acquisition within a few seconds, which, in turn, reduces laser-induced irreversible damage of the silver surface.[22,23] The excitation wavelengths used were 514.5 nm of an argon ion laser (Spectra Physics, 164−06) and 632.8 nm of a He−Ne laser (Research Electro-Optics, LHRP 2001). The laser power was maintained at 50 mW for the 514.5 nm line and 10 mW for the 632.8 nm line on the sample. The sample was mounted on a copper holder attached to a helium cryostat (Janis Research, CCS-600) inside the vacuum chamber maintained at 5×10^{-7} Torr. The annealing of the silver films was performed at 150 °C for 20, 50, and 70 min using a homemade heater in a vacuum. After being annealed, the silver films were dipped again in the ethanethiol solution and rinsed cleanly in order to maintain the constant coverage of ethanethiol on the film. Scanning electron micrographs of silver island films were taken with FE-SEM (JEOL JSM-6330F). To achieve high resolution, the silver surfaces were coated with ∼21 Å gold thin film using an ion sputter and the images were taken with a 15 kV acceleration voltage from an 8 mm working distance. All the AFM images were obtained in air using a Digital Instruments Nanoscope IIIa in tapping mode. Etched silicon tips with 5−10 nm height and ∼10 nm curvatures were used. The spring constant of cantilevers was about 50 N/m, and a resonance frequency of 300 kHz was used.

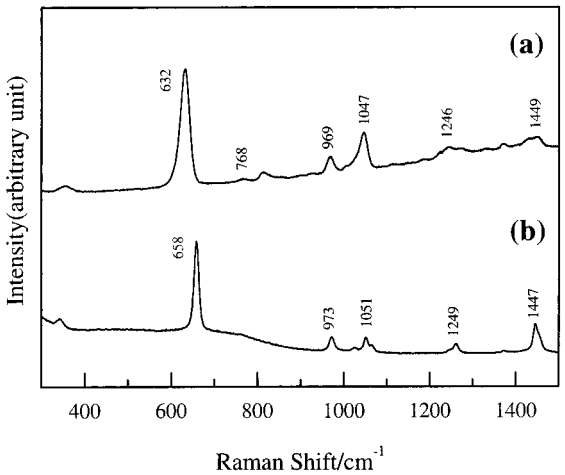

Figure 1. (a) SER spectrum of ethanethiol on silver film at 300 K and 1 atm and (b) ordinary Raman spectrum of ethanethiolate in basic aqueous solution.

3. Results and Discussion

The SER spectrum of ethanethiol adsorbed on a chemically prepared silver island film (shown in Figure 1a) is well correlated with the ordinary Raman spectrum of ethanethiolate in a basic solution (Figure 1b). The pattern of the observed SER spectrum is also similar to that obtained in the silver colloid solution by Joo et al.[24] Since a detailed spectral analysis has been reported previously,[24] only the results of the adsorption structure of ethanethiol on the silver film are briefly stated. The absence of an S−H stretching peak in the SER spectrum (2572 cm^{-1} for neat ethanethiol) suggests that ethanethiol adsorbs dissociatively on the silver film by losing its thiol proton. The resulting ethanethiolate binds to the silver surface via its S atom, evidenced by the large shift (∼26 cm^{-1}) in the frequency and the large increase (∼10 cm^{-1}) in the bandwidth of the SER C−S stretching peak (632 cm^{-1}) compared to the ordinary Raman C−S stretching peak (658 cm^{-1}). This trend of dissociative adsorption can be considered as a general feature for the adsorption of small alkanethiol molecules on the metal surfaces.[25,26]

As a continuing effort of our previous work,[16] we investigated the temperature dependence of SERS enhancements for ethanethiol adsorbed on annealed Ag island films. For this, the SERS intensity of the C−S stretching mode well isolated from other vibrational modes in frequency was monitored as functions of surface temperature and annealing time at two excitation wavelengths (514.5 and 632.8 nm). To keep ethanethiol coverage constant on various annealed films, the annealed films were redipped in the ethanethiol solution and subsequently rinsed in water prior to the SERS measurements. No thermal decomposition of adsorbed ethanethiol molecules due to annealing and laser irradiation was also ensured by no changes in the SER spectra. Moreover, the observed negligible changes in the SERS frequency and bandwidth of the C−S stretching mode for various annealing conditions suggested the constant adsorption geometry for ethanethiol molecules on various annealed films.

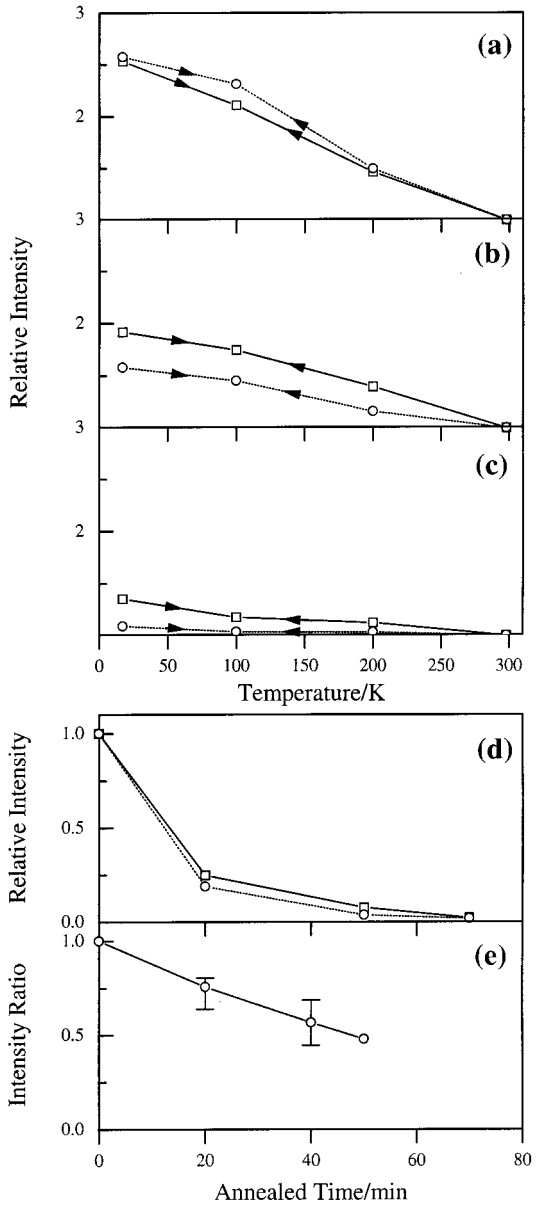

Figure 2. Temperature-dependent change in SERS intensity of the C−S stretching band of ethanethiol adsorbed on (a) the silver surface and on the silver surface annealed at 150 °C for (b) 20 min and (c) 50 min. Excitation wavelengths are 514.5 (−) and 632.8 (···) nm. (d) Relative decay and (e) $I_{632.8nm}/I_{514.5nm}$ ratio of SERS intensity are measured at 300 K for C−S stretching band as a function of annealing time.

It is believed that the observed changes in the SERS intensities for different surface temperatures and annealing conditions are unlikely due to the so-called chemical effects coming from the changes in the number and geometry of adsorbed ethanethiol molecules on the island surfaces but rather are due to the different EM enhancements for the different temperatures and morphologies of islands.

Parts a−c of Figure 2 show the reversible temperature dependence of the SERS intensities of the C−S stretching mode at 514.5 and 632.8 nm in the temperature range 15−300 K and at three annealing conditions: 0, 20, and 50 min of annealing at 150 °C. The SERS intensities of the C−S stretching mode were measured at various spots of the silver film for each temperature and each annealing condition and were then averaged. The observed results were verified by repeating the entire measurements for three or four other films. For unannealed films, as shown in Figure 2a, the C−S stretching intensities increase gradually for both wavelengths as the surface temperature decreases from 300 to 15 K, with the intensity at 15 K being larger than that at 300 K by a factor of ∼2.5. This temperature dependence was also reversible, similar to the case of 1-propanethiol adsorbed on chemical film.[16] In our previous work, these experimental findings were explained qualitatively by invoking the inherent temperature dependence of the EM enhancement. According to low-temperature-modified EM theory, a large SERS enhancement occurs when the surface plasmon resonance condition is satisfied for the real part of the dielectric function (ϵ) and at the same time the imaginary part of ϵ is small at the excitation wavelength. The observed temperature dependence of the SERS enhancement on a single silver island film (i.e., constant surface plasmon condition) was attributed to the fact that the imaginary part of ϵ (which appears in the denominator of the equation) is an increasing function of temperature in the range 10−300 K. The observed temperature dependence was well correlated with the calculated temperature dependence based on EM theory for the well-characterized distribution of Ag islands using FE-SEM and AFM techniques (which will be discussed later).

When the silver films were annealed for 20 min at 150 °C (Figure 2b), a similar temperature dependence but with much less enhancement compared to the case of unannealed film was found. Of notable importance is that the relative enhancement at 15 vs 300 K for 632.8 nm was more suppressed than those for 514.5 nm, suggesting that the annealing process could deteriorate greatly the morphologies of the silver islands for longer wavelength. The wavelength dependence was more marked for a 50 min annealed film with which almost a negligible temperature dependence of enhancement for 632.8 nm was found. These results are summarized in parts d and e of Figure 2 by plotting the relative SERS intensity normalized to that for unannealed film as a function of annealing time, and the ratios of these relative SERS intensities at 300 K for 632.8 nm vs 514.5 nm, respectively. Also to be noted in Figure 2d is that the relative enhancements at both wavelengths decreased rapidly during the first 20 min of annealing and then slowly thereafter.

To investigate the changes in the morphologies of silver islands induced by annealing, the FE-SEM and AFM images of unannealed and annealed films were taken. These are shown in Figures 3 and 4. These images are portions of wide surface images obtained before and after ∼1 h annealing at 150 °C. One notable thing in the FE-SEM images is that the annealing of the silver film increased the apparent size and number of silver islands because of the collapse of the individual island nanoparticles. The average radii of silver islands for unannealed and annealed films were 39 ± 1.5 and 43 ± 1.7 nm, respectively. The number of islands also increased by ∼10% for the annealed film compared to that of an unannealed film. The reason for the latter is believed to be that the reduced differences in the depths of islands for annealed films allowed a better microscopic view of the small silver islands that were invisible on an unannealed film. Similar changes in the morphologies of Ag islands were also seen in the AFM images (Figure 4). The observed average height of the islands from the AFM image for an unannealed film was $\sim 70 \pm 20$ nm, and for the annealed film it decreased by ∼10%. The observed size and height distributions of Ag islands on the chemical film in this work are similar to those of our previous report[16] and to those of the AFM studies by Pan and Phillips on chemically prepared silver films.[27] These FE-SEM and AFM studies confirmed that the

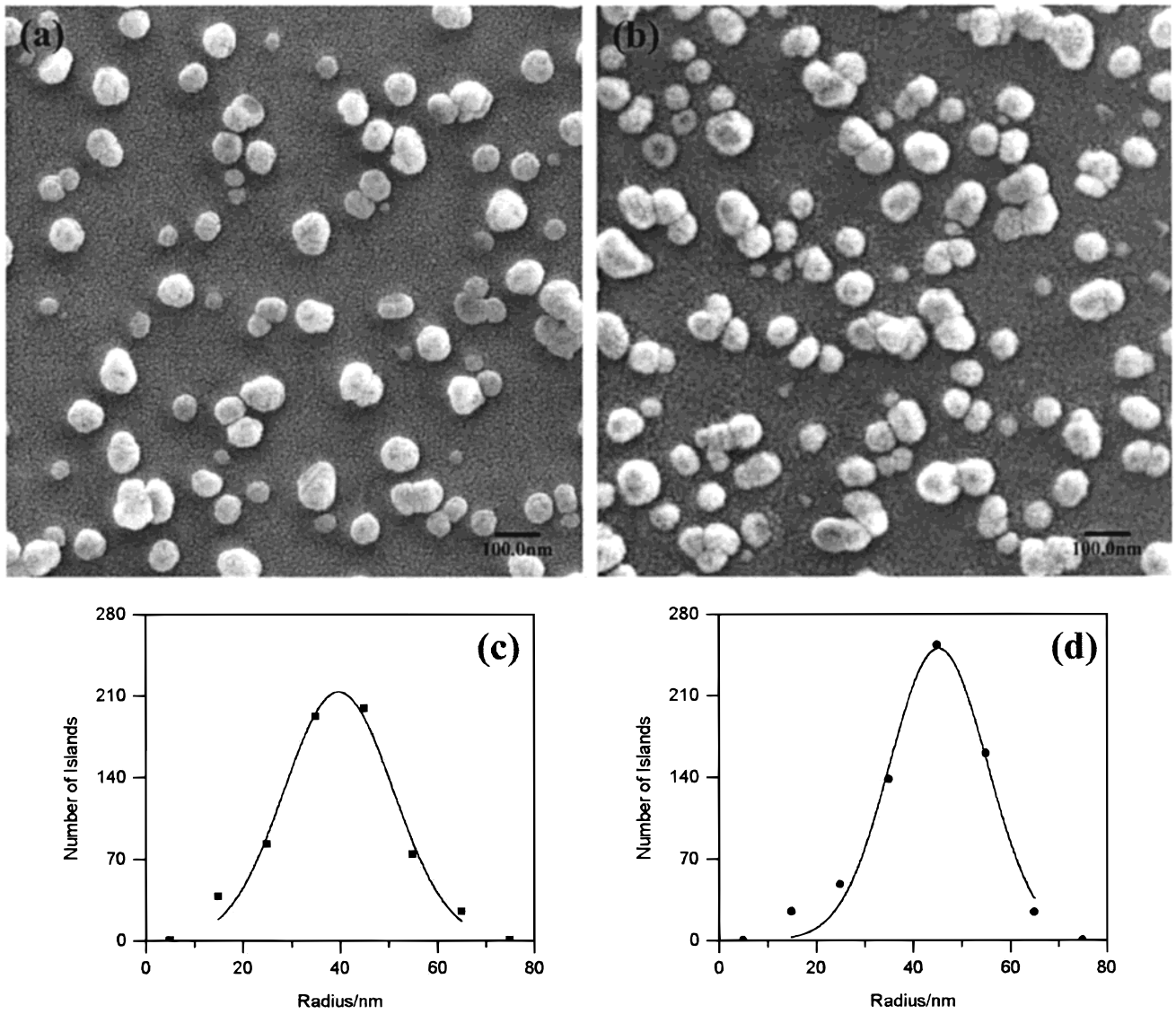

Figure 3. Field emission scanning electron micrographs of silver island films (a) before and (b) after 1 h of annealing at 150 °C (60000× magnification). The bar equals 100 nm. The distributions of the radii (or minor axis length *b*) of silver islands inside a ~25 μm^2 sampling area are shown (c) before and (d) after 1 h of annealing at 150 °C.

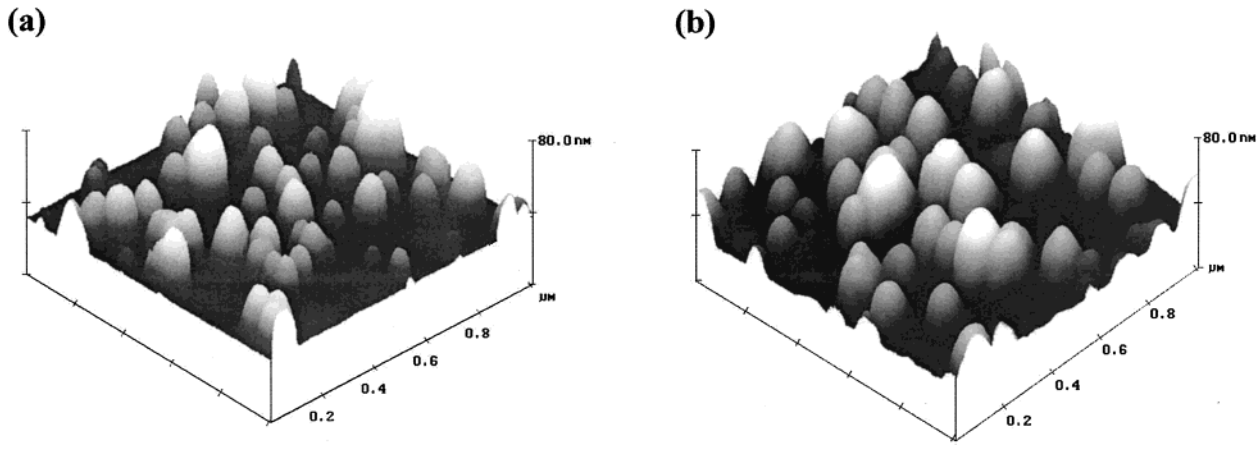

Figure 4. Atomic force micrographs of silver island films (a) before and (b) after 1 h of annealing at 150 °C. The scan size of the image obtained in tapping mode is 1 μm × 1 μm.

annealing of the chemical silver films modified the morphologies of the islands and that the aspect ratio (*a*/*b*) of effective hemispheroids decreased because of the combined results of increases in the radii and decreases in the heights of the islands.

The distributions of the *a*/*b* ratios for unannealed and annealed films can be estimated quantitatively from the radii of the islands in the FE-SEM images and the average heights of the islands in the AFM images, assuming effective hemispheroids for the

island particles. The distributions of the radii (or minor axis length b) of silver islands inside a ~25 μm^2 sampling area containing ~2000 islands before and after ~1 h of annealing were measured from the FE-SEM images, then fitted with single Gaussian functions as shown in parts c and d of Figure 3. Similarly, the averaged heights (or major axis length a) of the islands for unannealed and annealed films from the AFM images were also measured. Because of the large errors involved in the height determination, however, we calculated instead the aspect ratios of the silver islands for an unannealed film as the ratios of the average height (a = 70 nm) and the Gaussian distribution of the radii (b). Consequently, the distribution of the aspect ratios for an unannealed film has the form of an inverse Gaussian function. For annealed films, on the other hand, the aspect ratio distributions were calculated assuming that the annealing process induced changes only in the shapes of the hemispheroidal islands with no changes in their volumes (i.e., constant volume approximation). Under this approximation, the increases in the radii of islands are always accompanied by similar decreases in the heights of islands to keep the volume of the hemispheroid constant. Consequently, the ~10% increase in the radii due to ~1 h annealing shifted the maximum of the a/b distribution curve from 1.9 (unannealed film) to 1.4 (annealed film).

By use of the low-temperature-modified EM equation derived in the previous work,[15,16] the temperature dependence of SERS enhancement for the above a/b distributions at 514.5 and 632.8 nm excitations was simulated at the temperature range 15−300 K and for several percent increases in the radii of the islands (0, 5, 10, 12, 15, 20%). Parts a−c of Figure 5 show the selected results of the calculated temperature dependence for 0, 12, and 20% increases in the radii of the islands. The overall trends are in excellent agreement with the experimental findings shown in Figure 2. For example, the calculated EM enhancement increases as the temperature is lowered and decreases as the island radii increase, consistent with the experimental observations. Importantly, the observed rapid decrease in the temperature dependence for 632.8 nm compared to that for 514.5 nm was well reproduced in the calculated curves in parts d and e of Figure 5. Annealing affects SERS with 632.8 nm more than that with 514.5 nm because the optimum aspect ratio corresponding to the surface plasmon resonance condition is larger for the former than for the latter: 4.85 with 632.8 nm and 3.32 with 514.5 nm. Also interesting is that the calculated enhancements for both wavelengths decreased substantially for the first 5% size increase and then decreased gradually, similar to the experimental findings shown in parts d and e of Figure 2. The similar patterns suggested that the annealing time in the experiment is well-correlated with the percent radius increase of the island in theory, although the exact relationship needs to be further investigated. From the equation, it was found that the faster decay of enhancement during the early period of annealing was due to the fact that the effective number of Ag islands possessing the a/b values close to 3.32 for 514.5 nm and 4.85 for 632.8 nm (which are mainly responsible for the overall enhancement) changes nonlinearly with increasing annealing time or percent increase of island radius. This is the combined result of the EM enhancement curve having almost a singular nature at the optimum a/b values and the a/b distributions having the form of an inverse Gaussian function in which the population of the islands with large a/b ratios decays nonlinearly with increasing percent increase of radius.

The excellent agreement between experiment and theory strongly suggests that the reversible temperature dependence

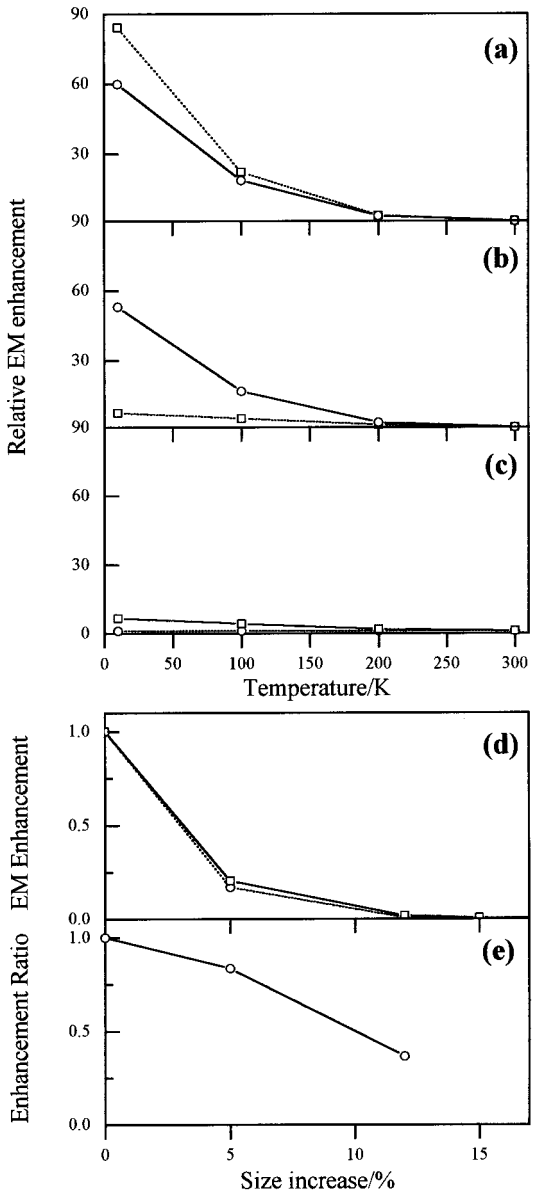

Figure 5. Relative EM enhancement for SERS at 514.5 (−) and 632.8 (···) nm excitation calculated as a function of temperature when the island size increased by (a) 0%, (b) 12%, and (c) 20%. The temperature dependence in EM enhancement averaged over a weighted distribution of the a/b ratio (1−6) is normalized to the value at 300 K. (d) The relative decay of EM enhancement and (e) $I_{632.8nm}/I_{514.5nm}$ ratio of EM enhancement are calculated at 300 K as a function of size increase.

of the SERS enhancement and the observed annealing effects could be explained within the framework of EM theory of SERS, particularly by using low-temperature-modified EM theory from the previous work. Some discrepancies in quantitatively comparing the theoretical predictions with the experimental findings, however, were found. First, the ratio of the calculated enhancements at 15 vs 300 K for an unannealed film was ~30 times higher than the corresponding experimental value (~2.5), although the mismatch between theory and experiment was much smaller than that in our previous work where constant a/b values were assumed. Second, the predicted percent increase in the radii of islands for a constant decay of the temperature dependence was higher than that of experiment, e.g. ~20% radius increase in theory vs ~10% radius increase for a 50 min annealed film in experiment. One of the most plausible explanations for these discrepancies is the overestimation of the a value due to large errors in determining the average height of

islands from the AFM images ($a = 70 \pm 20$ nm) and also due to the nonhemispheroidal nature of island particles.[28,29] Interestingly, when the lower limit of the average height ($a = 50$ nm) was used instead in the calculation, these discrepancies between experiment and theory was much reduced. The ratio of calculated enhancements at 15 vs 300 K was ~15 times higher than the experimental value, and the predicted percent increase in radius corresponding to ~10% radius increase in the experiment was ~13%. Other possible reasons for these discrepancies, as discussed previously,[16] could be in the inaccuracy of the optical data used in the calculation and the nonlocal effects of spheroidal islands,[30,31] resulting in a decrease in SERS enhancement at frequencies close to the surface plasmon frequency. More elaborate studies such as accurate measurements of the *a*/*b* distributions of Ag islands on the film and of the optical data for Ag island films are needed before the direct quantitative correlation between experiment and theory is realized. Recent SERS studies[12−14] on single molecules adsorbed on single Ag nanoparticles with well-characterized morphologies are one of the important contributions to progress in this direction. Nevertheless, the present experimental and theoretical endeavors provided better understanding of the intriguing aspect of SERS on the silver island film, i.e., reversible temperature dependence and the annealing effect in SERS.

In summary, we observed a reversible temperature dependence for the SERS intensities of ethanethiol adsorbed on a chemically prepared silver film with the intensity at 15 K being larger than that at 300 K by a factor of ~2.5, similar to the case of propanethiol. Importantly, the preferential enhancement of the SERS intensities at lower temperatures, normalized by the value at 300 K, decreased as the films was annealed. Such an attenuation of the SERS enhancement induced by annealing was more pronounced for a longer wavelength and during the early period of annealing. The FE-SEM and AFM studies revealed that the annealing process changed the morphologies of the silver islands such that the aspect ratios decreased somewhat because of the combined increases in the radii of the islands and decreases in their heights. By estimating the distributions of the aspect ratios of effective island hemispheroids for both unannealed and annealed films, we were able to reproduce successfully the experimentally observed temperature dependence and annealing effect using the low-temperature-modified EM theory. This combined experimental and theoretical work suggests once again the important role of EM theory in SERS phenomena, particularly for the temperature dependence and annealing effect in SERS. We hope that the results of this work will stimulate further theoretical and experimental studies of the SERS phenomena in controlled environments such as SERS on single Ag nanoparticles with optimally tailored morphologies.

Acknowledgment. This work was supported by Korea Research Foundation made in the program year 1998 (1998-015-D00158) and by the Specified Basic Research Fund of Korea Science and Engineering Foundation (KOSEF 94-0501-02-05-3).

References and Notes

(1) Fleischmann, M.; Hendra, P. J.; McQuillan, A. J. *Chem. Phys. Lett*. **1974**, *26*, 163.
(2) Chang, R. K.; Furtak, T. E. *Surface-Enhanced Raman Scattering*; Plenum: New York, 1982.
(3) Jiang, X.; Champion, A. *Chem. Phys. Lett*. **1987**, *140*, 95.
(4) Otto, A. *J. Raman Spectrosc*. **1991**, *22*, 743.
(5) Van Duyne, R. P.; Hulteen, J. C.; Treichel, D. A. *J. Chem. Phys*. **1993**, *99*, 2101.
(6) Roark, S. E.; Rowlen, K. L. *Chem. Phys. Lett*. **1993**, *212*, 50.
(7) Feofanov, A.; Ianoul, A.; Kryukov, E.; Maskevich, S.; Vasiliuk, G.; Kivach, L.; Nabiev, I. *Anal. Chem*. **1997**, *69*, 3731.
(8) Douketis, C.; Wang, Z.; Haskett, T. L.; Moskovits, M. *Phys. Rev. B* **1995**, *51*, 11022.
(9) Gimzewski, J. K.; Humbert, A.; Bednorz, J. G.; Reihl, B. *Phys. Rev. Lett.* **1985**, *55*, 951.
(10) Xiao, T.; Ye, Q.; Sun, L. *J. Phys. Chem. B* **1997**, *101*, 632.
(11) Royer, P.; Goudonnet, J. P.; Warmack, R. J.; Ferrell, T. L. *Phys. Rev. B* **1987**, *35*, 3753.
(12) Kneipp, K.; Wang, Y.; Kneipp, H.; Perelman, L. T.; Itzkan, I.; Dasari, R. R.; Feld, M. S. *Phys. Rev. Lett.* **1997**, *78*, 1667.
(13) Nie, S.; Emory, S. R. *Science* **1997**, *275*, 1102.
(14) Emory, S. R.; Haskins, W. E.; Nie, S. *J. Am. Chem. Soc.* **1998**, *120*, 8009.
(15) Chiang, H. P.; Leung, P. T.; Tse, W. S. *J. Chem. Phys*. **1998**, *108*, 2659.
(16) Pang, Y. S.; Hwang, H. J.; Kim, M. S. *J. Phys. Chem. B* **1998**, *102*, 7203.
(17) Leung, P. T.; Hider, M. H.; Sanchez, E. J. *Phys. Rev*. *B* **1996**, *53*, 12659.
(18) Gersten, J.; Nitzan, A. *J. Chem. Phys*. **1980**, *73*, 3023.
(19) McKay, J. A.; Rayne, J. A. *Phys. Rev*. *B* **1976**, *13*, 673.
(20) Biondi, M. A. *Phys. Rev*. **1956**, *102*, 964.
(21) Boo, D. W.; Oh, W. S.; Kim, M. S.; Kim, K.; Lee, H. C. *Chem. Phys. Lett*. **1985**, *120*, 301.
(22) Sobocinski, R. L.; Pemberton, J. E. *Langmuir* **1988**, *4*, 836.
(23) Kudelski, A.; Bukowska, J. *Spectrochim. Acta* **1995**, *51A*, 573.
(24) Joo, T. H.; Kim, K.; Kim, M. S. *J. Phys. Chem.* **1986**, *90*, 5816.
(25) Joo, T. H.; Kim, K.; Kim, M. S. *J. Mol. Struct.* **1987**, *158*, 265.
(26) Lee, S. B.; Kim, K.; Kim, M. S.; Oh, W. S.; Lee, Y. S. *J. Mol. Struct.* **1993**, *296*, 5.
(27) Pan, D.; Phillips, D. L. *Chem. Phys. Lett*. **1997**, *275*, 227.
(28) Nitzan, A.; Brus, L. E. *J. Chem. Phys*. **1981**, *75*, 2205.
(29) Leung, P. T. *Phys. Rev. B* **1990**, *42*, 7622.
(30) Leung, P. T.; Hider, M. H. *J. Chem. Phys*. **1993**, *98*, 5019.
(31) Fuchs, R.; Claro, F. *Phys. Rev. B* **1987**, *35*, 3722.